



Thermodynamic properties of ammonium magnesium sulfate hexahydrate $(\text{NH}_4)_2\text{Mg}(\text{SO}_4)_2 \cdot 6\text{H}_2\text{O}$

Daria A. Kosova*, Anna I. Druzhinina, Lyudmila A. Tiflova, Alla S. Monayenkova, Irina A. Uspenskaya

Chemistry Department, Lomonosov Moscow State University, Department of Chemistry, GSP-1, 1-3 Leninskiye Gory, Moscow 119991, Russian Federation

ARTICLE INFO

Article history:

Received 4 April 2017

Received in revised form 12 November 2017

Accepted 27 November 2017

Available online 2 December 2017

Keywords:

Heat capacity

Standard functions of formation

Phase transition

Adiabatic and solution calorimetry

Boussingaultite

ABSTRACT

Heat capacity of $(\text{NH}_4)_2\text{Mg}(\text{SO}_4)_2 \cdot 6\text{H}_2\text{O}$ (CAS: 7785-18-4) was measured by low-temperature vacuum adiabatic calorimetry (AC) in the temperature range from 8 to 320 K. A linear combination of Einstein functions was applied to approximate obtained data on the heat capacity. Heat content and entropy of $(\text{NH}_4)_2\text{Mg}(\text{SO}_4)_2 \cdot 6\text{H}_2\text{O}$ in the temperature range from 0 to 320 K were calculated from these data. The molar enthalpy of $(\text{NH}_4)_2\text{Mg}(\text{SO}_4)_2 \cdot 6\text{H}_2\text{O}$ dissolution in water was measured at 298.15 K by solution calorimetry (SC). Standard entropy, enthalpy of formation and Gibbs energy formation of $(\text{NH}_4)_2\text{Mg}(\text{SO}_4)_2 \cdot 6\text{H}_2\text{O}$ at 298.15 K were calculated from these results and literature data. Melting point of $(\text{NH}_4)_2\text{Mg}(\text{SO}_4)_2 \cdot 6\text{H}_2\text{O}$ was evaluated at external pressure 10^4 kPa by differential scanning calorimetry (DSC). The reversible phase transition of $(\text{NH}_4)_2\text{Mg}(\text{SO}_4)_2 \cdot 6\text{H}_2\text{O}$ crystal aggregates was recorded using three independent methods: DSC, AC and dielectric permittivity measurements. It was shown that this transition is absent for $(\text{NH}_4)_2\text{Mg}(\text{SO}_4)_2 \cdot 6\text{H}_2\text{O}$ having smaller crystal size obtained by grinding of the crystal aggregates in an agate mortar.

© 2017 Published by Elsevier Ltd.

1. Introduction

Investigation of the thermodynamic properties of ammonium magnesium sulfate hexahydrate $(\text{NH}_4)_2\text{Mg}(\text{SO}_4)_2 \cdot 6\text{H}_2\text{O}$ can be of economic and environmental interest. $(\text{NH}_4)_2\text{Mg}(\text{SO}_4)_2 \cdot 6\text{H}_2\text{O}$ exists as a mineral boussingaultite in the Earth's crust [1]. $(\text{NH}_4)_2\text{Mg}(\text{SO}_4)_2 \cdot 6\text{H}_2\text{O}$ is the main intermediate that is formed during the process of serpentinite ores autopsy ($\text{Mg}_3\text{Si}_2\text{O}_5(\text{OH})_4$) by ammonium sulfate as magnesium extractant [2]. This process is used in the metallurgical industry [3]. Highfield et al. [2] showed that this process can also be applied in the cycle of carbon dioxide capture and storage in the form of magnesite. $(\text{NH}_4)_2\text{Mg}(\text{SO}_4)_2 \cdot 6\text{H}_2\text{O}$ and its anhydrous salt (efremovite $(\text{NH}_4)_2\text{Mg}_2(\text{SO}_4)_3$) also may find application in agriculture because they contain macro- and meso-elements (N, S, Mg) required for the normal plants growth. It should be noted that potassium-containing analogous of efremovite – langbeinite $(\text{K})_2\text{Mg}_2(\text{SO}_4)_3$ is applied as a complex fertilizer in agriculture [4].

It is advisable to apply the methods of chemical thermodynamics and thermodynamic modeling for the determination of the optimal conditions of the various technological processes (temper-

ature, external pressure, the amount of the reagents) having the highest yield of the target product and the lowest energy consumption. It is necessary to possess information on the thermodynamic functions of all compounds involved into the reaction, including intermediates, to calculate the equilibrium composition of the system at each stage of the process.

Data on the thermodynamic properties of $(\text{NH}_4)_2\text{Mg}(\text{SO}_4)_2 \cdot 6\text{H}_2\text{O}$ is presented in the literature fragmentary. There is only information about the temperature and enthalpy of $(\text{NH}_4)_2\text{Mg}(\text{SO}_4)_2 \cdot 6.29\text{H}_2\text{O}$ melting determined by DSC at atmospheric pressure [5]. Voight et al. observed two peaks on the DSC curve and they related their to the incongruent melting of the compound. Both the peaks were characterized: $T_m^I = 397.2$ K, $\Delta H_m^I(T_m^I) = 41$ $\text{kJ} \cdot \text{mol}^{-1}$ and $T_m^{II} = 426.2$ K, $\Delta H_m^{II}(T_m^{II}) = 48$ $\text{kJ} \cdot \text{mol}^{-1}$. The total uncertainty of the enthalpy determination was 10%, but the uncertainty of the temperature determination wasn't specified in the text of the article. Moreover, it is not clear how the characteristic temperatures of the melting were determined, by the onset or by the extremum of the DSC peaks. In the literature there is information about theoretically predicted standard enthalpy of $(\text{NH}_4)_2\text{Mg}(\text{SO}_4)_2 \cdot 6\text{H}_2\text{O}$ formation $\Delta_f H_{m,298.15}^0 = -4270.3 \pm 26.0$ $\text{kJ} \cdot \text{mol}^{-1}$ [6]. On account of the above mentioned the aim of the present study was to obtain data on the thermodynamic properties of $(\text{NH}_4)_2\text{Mg}(\text{SO}_4)_2(\text{H}_2\text{O})_6$: (1) measurements of the heat capacity $C_{p,m}(T)$ in a wide temperature range; (2) determination of the salt

* Corresponding author.

E-mail addresses: ira@td.chem.msu.ru (D.A. Kosova), druzhinina@thermo.chem.msu.ru (A.I. Druzhinina), tiphlova@phys.chem.msu.ru (L.A. Tiflova), monal@phys.chem.msu.ru (A.S. Monayenkova), ira@td.chem.msu.ru (I.A. Uspenskaya).

dissolution enthalpy in water; (3) calculation of the entropy $S_m^0(T)$ and heat content ($H_m^0(T) - H_m^0(0)$); (4) calculation of the standard enthalpy $\Delta_f H_m^0$, entropy $\Delta_f S_m^0$ and Gibbs energy of formation at 298.15 K; (5) estimation of the phase transition parameters.

2. Materials

2.1. Synthesis of samples

Commercial reagents without additional purification (characterization of the compounds is given in Table 1) and distilled water were used in the synthesis of $(\text{NH}_4)_2\text{Mg}(\text{SO}_4)_2 \cdot 6\text{H}_2\text{O}$.

On the basis of the data about solid–liquid phase equilibria in the system $\text{MgSO}_4 - (\text{NH}_4)_2\text{SO}_4 - \text{H}_2\text{O}$ [7–10] the following conditions of $(\text{NH}_4)_2\text{Mg}(\text{SO}_4)_2 \cdot 6\text{H}_2\text{O}$ synthesis were applied. Mixtures of 4.164 g $(\text{NH}_4)_2\text{SO}_4$, 7.780 g $\text{MgSO}_4 \cdot 7\text{H}_2\text{O}$ and 18.056 g H_2O were maintained under stirring at $338 \div 343$ K until complete dissolution of salts. Reagents were weighted on an AXIS AG300 balance with an expanded uncertainty ($k = 2$) of the mass determination $U = 0.001$ g. Vessel with a solution was tightly closed and was kept at a room temperature for night. Crystals began to grow immediately during the cooling of the solution. Obtained crystals having the average dimensions about 1 cm (Fig. 1) were decanted from the mother liquor and were dried on air.

In the present study crystals of $(\text{NH}_4)_2\text{Mg}(\text{SO}_4)_2 \cdot 6\text{H}_2\text{O}$ with the different morphology were investigated, namely, the crystal aggregates formed during the synthesis (Fig. 1) without additional preparation and these crystals milled into an agate mortar under a minimal mechanical influence (powdered crystals). Crushing of the crystal aggregates was carried out each time just before the experiment.

Table 1
Purities and sources of chemicals.

Chemical name	CAS number	Source	Purity/mass fraction
$(\text{NH}_4)_2\text{SO}_4$	7783-20-2	«Irea2000»	≥ 0.99
$\text{MgSO}_4 \cdot 7\text{H}_2\text{O}$	10034-99-8	«Merck»	≥ 0.995
$(\text{NH}_4)_2\text{Mg}(\text{SO}_4)_2 \cdot 6\text{H}_2\text{O}$	7785-18-4	Synthesis	≥ 0.998



Fig. 1. Crystal aggregates of $(\text{NH}_4)_2\text{Mg}(\text{SO}_4)_2 \cdot 6\text{H}_2\text{O}$ obtained during the synthesis.

2.2. Characterization of sample

Crystals of $(\text{NH}_4)_2\text{Mg}(\text{SO}_4)_2 \cdot 6\text{H}_2\text{O}$ obtained in the present study were subjected to chemical, DSC and XRD (X-ray diffraction) analysis. It was revealed that the crystals consist of a boussingaultite $(\text{NH}_4)_2\text{Mg}(\text{SO}_4)_2 \cdot 6\text{H}_2\text{O}$ single phase by comparison of theoretical [11] and experimental diffraction patterns (Fig. 2). It was shown that the crystals do not contain free ammonium sulfate, because the DSC peak corresponding to the phase transition of ammonium sulfate at 223 K [12] is absent on the experimental curve (Fig. 3). Magnesium Mg^{2+} in the sample was determined by the complexometric titration with EDTA. Ammonium NH_4^+ group quantity was evaluated by Sorensen formol titration. Sulfate SO_4^{2-} group quantity was determined as barium sulfate using gravimetry. Water content in the salt was evaluated by weighting of the substance before and after annealing in a furnace to constant weight of the sample at 373 K. Results of $(\text{NH}_4)_2\text{Mg}(\text{SO}_4)_2 \cdot 6\text{H}_2\text{O}$ chemical analysis are summarized in Table 2.

3. Experimental methods

3.1. Low-temperature vacuum adiabatic calorimetry (AC)

The heat capacity of the $(\text{NH}_4)_2\text{Mg}(\text{SO}_4)_2 \cdot 6\text{H}_2\text{O}$ was measured with the help of a automated vacuum adiabatic calorimeter in

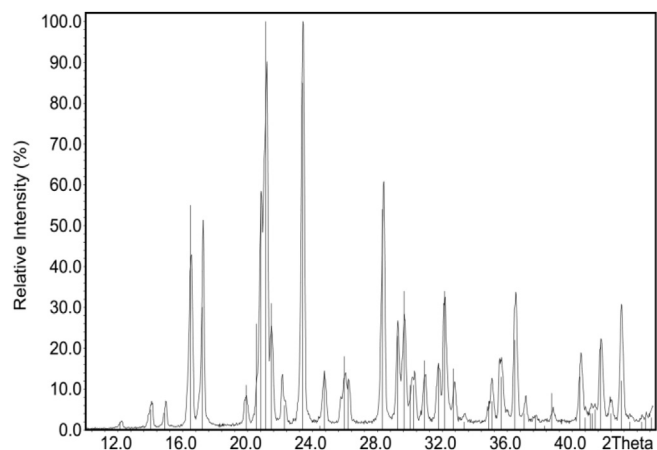


Fig. 2. Diffraction pattern of $(\text{NH}_4)_2\text{Mg}(\text{SO}_4)_2 \cdot 6\text{H}_2\text{O}$ powdered crystals. Solid line – experimental data; strong peaks (vertical lines) – literature data (ICDD 35-771) [11].

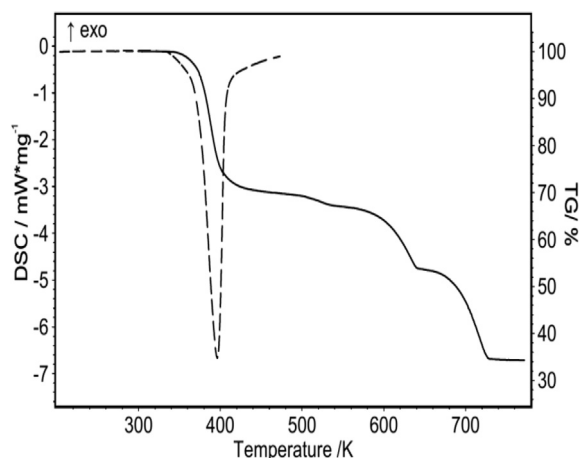


Fig. 3. TGA (solid line) and DSC (dashed line) curves of $(\text{NH}_4)_2\text{Mg}(\text{SO}_4)_2 \cdot 6\text{H}_2\text{O}$ powdered crystals. Heating rate is $10 \text{ K} \cdot \text{min}^{-1}$.

Table 2Chemical analysis of $(\text{NH}_4)_2\text{Mg}(\text{SO}_4)_2 \cdot 6\text{H}_2\text{O}$ (The molar mass of the $(\text{NH}_4)_2\text{Mg}(\text{SO}_4)_2 \cdot 6\text{H}_2\text{O}$ is $360.61 \text{ g}\cdot\text{mol}^{-1}$).^{a,b}

Particle	Experimental/mass fraction ^c	$U(\text{mass fraction})^c$	Theoretical/mass fraction	Morphology of the sample	Method
Mg^{2+}	0.0673	0.0004	0.0674	crystal aggregates	Titration
NH_4^+	0.0999	0.0004	0.1000	crystal aggregates	Titration
SO_4^{2-}	0.5333	0.0007	0.5328	crystal aggregates	Gravimetry
H_2O	0.2994	0.0005	0.2998	powdered crystals	Gravimetry
H_2O	0.2995	0.001	0.2998	crystal aggregates	Indirect determination from data of lines 1–3

^a Expanded uncertainty $U(k=2)$ is $U(\text{Molar Mass}) = 0.3 \text{ g}\cdot\text{mol}^{-1}$ were estimated from the data of chemical analysis.^b Molar mass was calculated using relative atomic masses recommended by IUPAC [13] taking into account the recommendation of [14].^c Expanded uncertainties $U(k=2)$ of the experimental data were evaluated by triple repetition of the analytical experiment.

the temperature range from 8 to 320 K. Liquid helium and nitrogen were applied as a refrigerants. Detailed description of the device configuration and calorimetric technique were done by Varushchenko et al. [15]. The instrument consists of vacuum adiabatic calorimeter, data acquisition and control system. The heat capacity was measured in a heating mode with the step $\Delta T \sim 1 \text{ K}$. The temperature of the calorimeter was registered by means of Fe-Rh resistance thermometer ($R_{273.1} \approx 50$) with a sensitivity $\pm 0.005 \text{ K}$. To reduce the ballast heat capacity of calorimeter the thermometer is located on an adiabatic shell. The temperature gradient between container and adiabatic shield was controlled with four-junction (Cu + 0.1 mass% Fe) chromel thermocouple with a sensitivity $\pm 0.003 \text{ K}$. The measurements were performed at $p_{298}(\text{He})/\text{kPa} = (10 \pm 2)$ in the container with the sample (helium was as the thermal exchange gas). High vacuum inside the calorimetric cell was kept by means of cry-sorption provided with an efficient charcoal getter.

The heat capacity of $(\text{NH}_4)_2\text{Mg}(\text{SO}_4)_2 \cdot 6\text{H}_2\text{O}$ was measured at the saturated vapor pressure ($C_{\text{sat,m}}$). We are unable to estimate the difference ($C_{\text{p,m}} - C_{\text{sat,m}} = T \left(\frac{\partial V}{\partial T}\right)_p \cdot \left(\frac{\partial p}{\partial T}\right)_{\text{sat}}$ in case of $(\text{NH}_4)_2\text{Mg}(\text{SO}_4)_2 \cdot 6\text{H}_2\text{O}$ due to the lack of appropriate experimental data. This difference was estimated for various classes of liquid and solid compounds for which there is data on the temperature dependencies of the density and vapor pressure. It was shown that this difference ($C_{\text{p,m}} - C_{\text{sat,m}}$) is less than uncertainties of experimental $C_{\text{sat,m}}$ data [15]. In the present study we have not taken into account ($C_{\text{p,m}} - C_{\text{sat,m}}$) for $(\text{NH}_4)_2\text{Mg}(\text{SO}_4)_2 \cdot 6\text{H}_2\text{O}$.

The masses of the investigated samples were determined by a Mettler balance and were in the range 0.5000–0.5500 g. Expanded uncertainty ($k=2$) of mass determination is $U = 5 \cdot 10^{-5} \text{ g}$. The volume of the container in which investigated samples were placed was 1 cm^3 . The calorimeter was tested with a high-pure Cu (99.995 mass%) and chromatographically pure *n*-heptane. Maximum deviations of the experimental data from the precision literature data [16,17] were not exceeded 2% in the range 8–80 K and 0.3% above 80 K. The total uncertainty of the container temperature determination was estimated $\pm 0.02 \text{ K}$ within the whole range of temperatures (8–320 K).

In the present study two type of $(\text{NH}_4)_2\text{Mg}(\text{SO}_4)_2 \cdot 6\text{H}_2\text{O}$ crystals were investigated with the different morphology (see «Materials»). Measurements were performed once in the temperature range 8–80 K for each type of crystals, and in the temperature range 80–320 K the experiment was repeated three times. The calculation of the thermodynamic functions was carried out according to the results of the third measurement.

3.2. Solution calorimetry

The measurements were performed at $T = 298.15 \text{ K}$ in sealed swinging calorimeter with an isothermal jacket, similar to that described in [18,19]. The temperature increase in experiments was measured with a platinum resistance thermometer ($R_{298.15} = 401.32 \Omega$, 1Ω corresponds to $\Delta T = 0.94 \text{ K}$) incorporated in the

bridge circuit, the its thermometric sensitivity was $3 \cdot 10^{-5} \text{ K}$. The energy equivalent of the calorimetric system filled with $(80.000 \pm 0.003) \text{ g}$ of H_2O is equal to $(322.62 \pm 0.23) \text{ J}\cdot\Omega^{-1}$. The calorimeter was tested several times by the dissolution of KCl in water (the molality of final solution was $0.028 \text{ mol}\cdot\text{kg}^{-1}$). The most recent set of KCl dissolution measurements yielded $(17.40 \pm 0.04) \text{ kJ}\cdot\text{mol}^{-1}$. The critically evaluated value is $(17.43 \pm 0.02) \text{ kJ}\cdot\text{mol}^{-1}$ [20]. The sample was placed into thin-walled glass ampoule and weighted on SARTORIUS balance with an expanded uncertainty ($k=2$) of the mass determination $U = 2 \cdot 10^{-5} \text{ g}$.

3.3. Differential scanning calorimetry (DSC)

DSC curves at atmospheric pressure were recorded by a NETZSCH DSC 204 F1 in a stream of N_2 at flow rate $40 \text{ ml}\cdot\text{min}^{-1}$ with the heating rate $10 \text{ K}\cdot\text{min}^{-1}$. DSC experiments under external pressure (10^4 kPa) were received by a NETZSCH DSC 204 HP. All measurements under external pressure were conducted in a stream of Ar at the flow rate $40 \text{ ml}\cdot\text{min}^{-1}$ with the heating rate $10 \text{ K}\cdot\text{min}^{-1}$. Maximum temperature interval of the DSC measurements was 123–773 K. Calibration procedure of the instruments was described in [12]. Specimens with the weight about $3\text{--}5 \cdot 10^{-3} \text{ g}$ were tested in aluminum crucibles (volume is 56 mm^3 , diameter is 6 mm) with pierced lid. Samples for DSC experiments were weighed on an analytical balance A&D GH-202 with an expanded uncertainty ($k=2$) of the mass determination is $U = 1 \cdot 10^{-5} \text{ g}$. Thermo-analytical curves were processed by means of the NETZSCH Proteus Analysis software. Experimental and computational procedures for DSC were performed according to standards ASTM E-793 and ASTM E-794.

3.4. Thermogravimetry (TGA)

TGA curves were recorded by NETZSCH TG 209 F1 in the temperature range 303–773 K for the estimation of the compounds thermal stability. Heating rate of experiments was $10 \text{ K}\cdot\text{min}^{-1}$. All measurements were conducted in a stream of N_2 at the flow rate $40 \text{ ml}\cdot\text{min}^{-1}$. Calibration technique of instrument was the same as described in [21]. Sample preparation in TGA was the same to the one in DSC experiments.

3.5. X-ray powder diffraction (XRD)

XRD data were obtained on a diffractometer Rigaku Miniflex 600. Angle 2θ was varied in the range from 10 to 60 in steps of 0.02; the exposure time was 10 s per point. Sample of $(\text{NH}_4)_2\text{Mg}(\text{SO}_4)_2 \cdot 6\text{H}_2\text{O}$ powdered crystals was identified by comparing theoretical [11] and experimental diffractograms.

3.6. Dielectric permittivity

Dielectric permittivity of $(\text{NH}_4)_2\text{Mg}(\text{SO}_4)_2 \cdot 6\text{H}_2\text{O}$ was investigated as a function of temperature $\epsilon_r(T)$ at frequency 1000 Hz

applying capacitance bridge Andeen Hagerling 2700H. Liquid nitrogen was used as a refrigerant. Measurements were done in the heating mode with the rate $10 \text{ K}\cdot\text{min}^{-1}$. Sample preparation was carried out in such way as it is described in [22]. Measurements were performed at the Department of Low Temperature Physics and Superconductivity of Lomonosov MSU.

4. Results and discussion

4.1. Thermal stability and melting point of $(\text{NH}_4)_2\text{Mg}(\text{SO}_4)_2\cdot 6\text{H}_2\text{O}$

The thermal stability of $(\text{NH}_4)_2\text{Mg}(\text{SO}_4)_2\cdot 6\text{H}_2\text{O}$ at atmospheric pressure was evaluated by TGA and DSC at the heating rate $10 \text{ K}\cdot\text{min}^{-1}$. Results of experiment are presented in Fig. 3. According to the results of the TGA the onset temperature of $(\text{NH}_4)_2\text{Mg}(\text{SO}_4)_2\cdot 6\text{H}_2\text{O}$ thermal decomposition was about $T_d \sim 340 \text{ K}$. As can be seen from Fig. 3 DSC curve have one endothermic peak in the range of temperatures 340–470 K which is associated with the thermal decomposition of the substance. We believe that values of T_m and $\Delta H_m(T_m)$ determined by Voight et al. for $(\text{NH}_4)_2\text{Mg}(\text{SO}_4)_2\cdot 6.29\text{H}_2\text{O}$ [5] are doubtful, because effect of water elimination is superimposed on the melting process under similar experimental conditions.

We conducted additional DSC experiments at external pressure 10^4 kPa to properly evaluate the melting point of $(\text{NH}_4)_2\text{Mg}(\text{SO}_4)_2\cdot 6\text{H}_2\text{O}$. Results of the experiments are presented in Fig. 4. DSC curve of $(\text{NH}_4)_2\text{Mg}(\text{SO}_4)_2\cdot 6\text{H}_2\text{O}$ has 5 peaks which is probably related to the following processes. Endothermic processes (1) and (2) are incongruently melting of the hydrate. The mass loss is not occurred in this range of temperatures unlike experiments at normal pressure. It is confirmed by check weighing of crucible with the sample after heating up to 440 K at 10^4 kPa . Peaks (1) and (2) on DSC curve are reproducible during thermal cycling. Due to changes of phase composition at lowering of pressure from 10^4 to 10^2 kPa , it is impossible to determine the composition of the liquid and solid phases formed during the melting of the hydrate in the DSC cell. Widened endothermic peak (3) corresponds to the evaporation of water from crucible. Exothermic process (4) is connected with the efremovite $\text{Mg}_2(\text{NH}_4)_2(\text{SO}_4)_3$ formation. These data agree with the results of work [3]. Small endothermic peak (5) at 637 K is related to the high-temperature phase transition of ammonium sulfate [12], that did not react with magnesium sulfate due to

the different stoichiometry between ammonium and magnesium cations in the structures of $(\text{NH}_4)_2\text{Mg}(\text{SO}_4)_2\cdot 6\text{H}_2\text{O}$ and of $\text{Mg}_2(\text{NH}_4)_2(\text{SO}_4)_3$. The amount of chemically free ammonium sulfate was estimated from the ratio of thermal effects between literature data [12] on the enthalpy of the phase transition at 637 K and area of the peak (5) on the DSC curve (Fig. 4). According to the results of these experiments during the heating of $(\text{NH}_4)_2\text{Mg}(\text{SO}_4)_2\cdot 6\text{H}_2\text{O}$ elimination of water is occurred and efremovite and ammonium sulfate in the solid residue are remained in a molar ratio of 1:1. This data are in a good agreement with the results of the XRD analysis of the solid products of $(\text{NH}_4)_2\text{Mg}(\text{SO}_4)_2\cdot 6\text{H}_2\text{O}$ thermal decomposition. Reflexes corresponding to phase of ammonium sulfate and efremovite are presented in the diffraction pattern (Fig. 5).

Incongruent melting point of $(\text{NH}_4)_2\text{Mg}(\text{SO}_4)_2\cdot 6\text{H}_2\text{O}$ at $P = 10^4 \text{ kPa}$ (Expanded uncertainty $U(k=2)$ of P is 100 kPa) was evaluated on the basis of 5 independent experiments; $T_m = 405 \pm 1 \text{ K}$ (Expanded uncertainty $U(k=2)$ of T_m is 1 K).

4.2. Heat capacity and phase transition of $(\text{NH}_4)_2\text{Mg}(\text{SO}_4)_2\cdot 6\text{H}_2\text{O}$

In the present work heat capacity $C_{p,m}(T)$ of $(\text{NH}_4)_2\text{Mg}(\text{SO}_4)_2\cdot 6\text{H}_2\text{O}$ was measured by means of AC from 8 to 320 K. We investigated both the crystal aggregates formed during the synthesis (Fig. 1) and these crystals grinded into an agate mortar under minimal mechanical influence (powdered crystals). Obtained experimental data of the $(\text{NH}_4)_2\text{Mg}(\text{SO}_4)_2\cdot 6\text{H}_2\text{O}$ heat capacity are given in Supplementary materials (Tables) and in Fig. 6.

We also detected phenomenon that occurs with the crystal aggregates of $(\text{NH}_4)_2\text{Mg}(\text{SO}_4)_2\cdot 6\text{H}_2\text{O}$ by means of three independent methods: DSC, relative permittivity measurements and AC. There are anomalies for crystal aggregates of $(\text{NH}_4)_2\text{Mg}(\text{SO}_4)_2\cdot 6\text{H}_2\text{O}$ on DSC (Fig. 7), dielectric permittivity (Fig. 8) and heat capacity curves (Fig. 6) at $T_{tr} = 270.6 \pm 0.4 \text{ K}$ (Expanded uncertainty $U(k=2)$ of T_{tr} is 0.4 K), which are reproduced during thermal cycling. These anomalies are absent for powdered crystals having a smaller crystallite size compared to crystal aggregates of $(\text{NH}_4)_2\text{Mg}(\text{SO}_4)_2\cdot 6\text{H}_2\text{O}$ (see «*synthesis of samples*»). It is quite rare and unusual phenomenon but some authors have observed one for various substances [23–26]. Unfortunately, calorimetric measurements are insufficient to reveal the nature of the phase transition. However, we can assume that this phase transition is associated with the appearance of the ferroelectric properties of the material (crys-

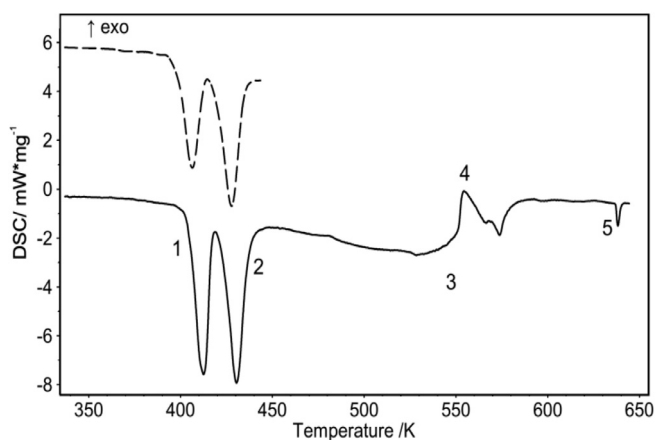


Fig. 4. DSC curves obtained under external pressure 10^4 kPa of $(\text{NH}_4)_2\text{Mg}(\text{SO}_4)_2\cdot 6\text{H}_2\text{O}$ powdered crystals. Dashed line correspond to the first heating of the sample; solid line – second heating. (1) and (2) are incongruent melting of $(\text{NH}_4)_2\text{Mg}(\text{SO}_4)_2\cdot 6\text{H}_2\text{O}$; (3) is evaporation of water; (4) is formation of efremovite; (5) phase transition of ammonium sulfate. Heating rate is $10 \text{ K}\cdot\text{min}^{-1}$. powdered crystals of $(\text{NH}_4)_2\text{Mg}(\text{SO}_4)_2\cdot 6\text{H}_2\text{O}$ were used in this experiment.

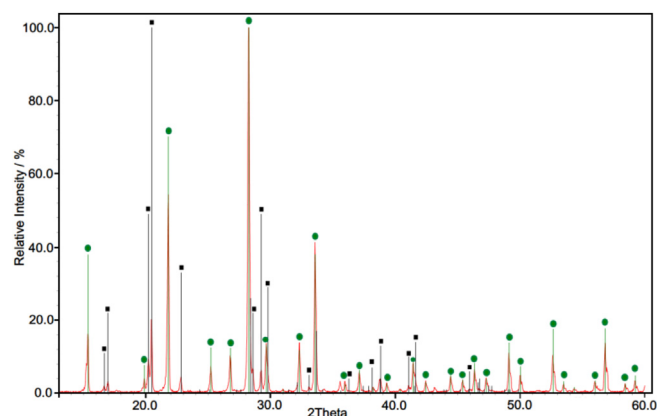


Fig. 5. Diffraction pattern of the $(\text{NH}_4)_2\text{Mg}(\text{SO}_4)_2\cdot 6\text{H}_2\text{O}$ decomposition products. Red line – experimental data; green lines and ● – efremovite (ICDD 42–1432); black lines and ■ – ammonium sulfate (ICDD 40–660) [11]. (For interpretation of the references to colour in this figure caption, the reader is referred to the web version of this article.)

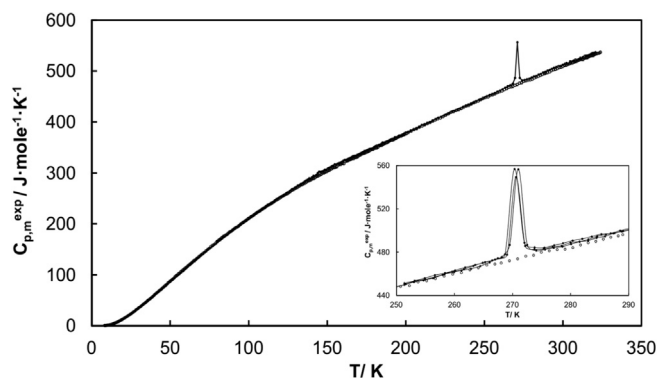


Fig. 6. The temperature dependence of the molar heat capacity of $(\text{NH}_4)_2\text{Mg}(\text{SO}_4)_2 \cdot 6\text{H}_2\text{O}$. Symbols correspond to the experimental data: ● – crystal aggregates obtained during the synthesis; ○ – powdered crystals. Solid line is the spline of the experimental data in the range of the phase transition.

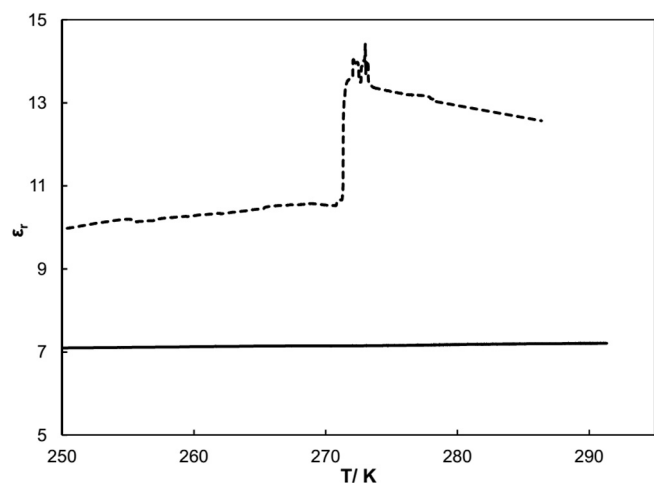


Fig. 7. Results of the $(\text{NH}_4)_2\text{Mg}(\text{SO}_4)_2 \cdot 6\text{H}_2\text{O}$ relative permittivity measurements. Dashed line – crystal aggregates obtained during the synthesis; solid line – powdered crystals. Frequency of the electromagnetic field is 1000 Hz; Heating rate is 10 $\text{K} \cdot \text{min}^{-1}$.

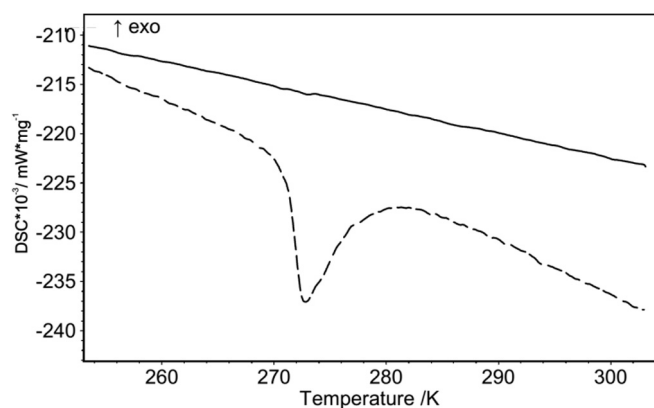


Fig. 8. Fragment of DSC curves of two $(\text{NH}_4)_2\text{Mg}(\text{SO}_4)_2 \cdot 6\text{H}_2\text{O}$ samples. Dashed line – crystal aggregates obtained during the synthesis; solid line – powdered crystals. Heating rate is 10 $\text{K} \cdot \text{min}^{-1}$.

tal aggregates) according to the dielectric permittivity measurements (Fig. 8). It was shown by authors of [22] that such transitions are very sensitive to the shape and grain size of the crystals. Information was found in the literature about orienta-

tional phase transition of C_{60} that characteristics and existence depend on the size of the crystallites [24,25]. According to [26] high-order superlattices in orientally ordered C_{60} exist; crystals of C_{60} having a smaller size than the superlattice do not have orientational phase transition. It was reliably discovered that leonite-type crystals $\text{K}_2\text{Mg}(\text{SO}_4)_2 \cdot 4\text{H}_2\text{O}$ undergo an order-disorder phase transition at 269 K [27]. The crystals change the symmetry from the disordered $C2/m$ to the oriented $I2/a$. To date, the crystal structure of $(\text{NH}_4)_2\text{Mg}(\text{SO}_4)_2 \cdot 6\text{H}_2\text{O}$ was studied only at room temperature [11]. Additional researches at low temperatures by other methods are needed for determination of the nature of $(\text{NH}_4)_2\text{Mg}(\text{SO}_4)_2 \cdot 6\text{H}_2\text{O}$ crystal aggregates phase transition and for establishing relationships between the presence of the phase transition and the crystallite size.

4.3. Thermodynamic functions of $(\text{NH}_4)_2\text{Mg}(\text{SO}_4)_2 \cdot 6\text{H}_2\text{O}$

A linear combination of Einstein functions (Eq. (1)) was applied to approximate the results of the heat capacity measurements. Thermodynamic foundation of the $C_{p,m}$ vs. T description by these functions was discussed in detail by Voronin and Kutsenok [28] as well as the advantages of this method compared with polynomial models. It should be noted that θ_i are variable parameters, which, in this case, do not have a strict physical meaning. Experimental data over the entire temperature range can be fitted to Eq. (1) by a single set of parameters. The entropy $S_m^0(T)$ and heat content $(H_m^0(T) - H_m^0(0))$ at any given temperature T (Eqs. (2) and (3), respectively) can be calculated analytically, i.e., the question of agreement of the thermodynamic data is solved:

$$C_{p,m}(T) = 3R \sum_i a_i \frac{(\frac{\theta_i}{T})^2 e^{\frac{\theta_i}{T}}}{(e^{\frac{\theta_i}{T}} - 1)^2} \quad (1)$$

$$S_m^0(T) = 3R \sum_i a_i \left(\frac{\theta_i/T}{e^{\theta_i/T} - 1} - \ln(1 - e^{-\theta_i/T}) \right) \quad (2)$$

$$(H_m^0(T) - H_m^0(0)) = 3RT \sum_i a_i \frac{(\theta_i/T)}{e^{\theta_i/T} - 1} \quad (3)$$

Unknown parameters a_i and θ_i of Eq. (1) were determined by the solution of the system of the nonlinear equations by the method of least squares using software «Cpfit» developed in the Laboratory of Chemical Thermodynamics of Lomonosov MSU and available at site [29].

Molar heat capacity of crystal aggregates and powdered crystals in the investigated temperature range have the same character (Figs. 6, 9); but average relative deviation between the heat capac-

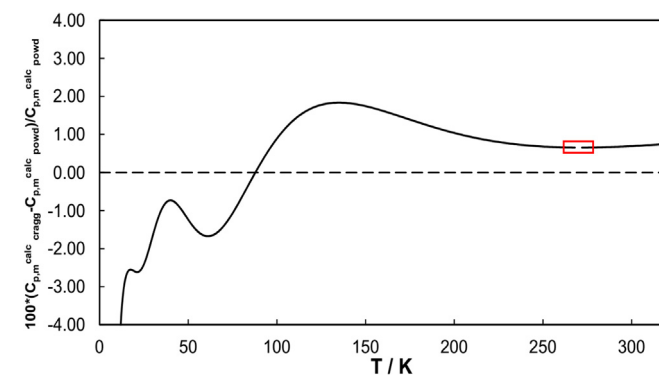


Fig. 9. Relative deviation between calculated by Eq. (1) molar heat capacities of crystal aggregates ($C_{p,m,calc}$) and of powdered crystals ($C_{p,m,calc_powd}$) $(\text{NH}_4)_2\text{Mg}(\text{SO}_4)_2 \cdot 6\text{H}_2\text{O}$. The function in the region of the phase transition was cut out from the graph.

Table 3

The calculated values of parameters (α_i , θ_i) in Eq. (1) those approximate the experimental heat capacity of $(\text{NH}_4)_2\text{Mg}(\text{SO}_4)_2 \cdot 6\text{H}_2\text{O}$ powdered crystals.

i	α_i	$U(\alpha_i)^a$	θ_i / K	$U(\theta_i)^a / \text{K}$
1	7.43786	1	560.73	63
2	17.1836	0.5	1334.17	58
3	0.0332639	0.006	14.9865	5
4	3.90846	1	170.478	14
5	5.60789	0.7	299.727	46
6	1.73241	0.1	84.3843	2

^a $U(\alpha_i)$ and $U(\theta_i)$ are expanded uncertainties ($k = 2$) of parameters α_i and θ_i .

ities of two samples is 1.2%. Moreover, it should be noted that this difference in the helium region (8–80 K) is comparable to the uncertainty of the method (2%), while in the nitrogen region (80–320 K) this difference is higher than the uncertainty of the method (0.3%), maximum deviation is 1.8% at 136 K. It should be noted that heat capacity of crystal aggregates is systematically higher than powdered crystals.

Existence of the difference between the heat capacities of crystal aggregates and powdered crystals may be due to the following reasons: (1) slight difference in the chemical composition of the samples; (2) reduction of the number of stresses and defects in the structure of the sample when the crystal aggregates are milled to powdered crystals. The first reason is unlikely, since the same sample before and after milling was investigated by adiabatic calorimetry. This procedure was repeated three times with different samples and gave similar results. The probable cause of the results discrepancy between the heat capacities measurements of samples with different morphology is related to the following. Since the crystalline aggregates are the splices of several crystal grains, the defects and stresses are present at the joint sites, this inevitably affects to the increasing of the Gibbs energy of the system and as a consequence to its heat capacity. The phase having a smaller number of defects is formed during the milling the crystal aggregates to powdered crystals, since the destruction primarily takes place in the joint sites of different grains of crystal aggregates with the formation of individual crystallites. In this connection, the thermodynamic functions of $(\text{NH}_4)_2\text{Mg}(\text{SO}_4)_2 \cdot 6\text{H}_2\text{O}$ were calculated from the heat capacity data of powdered crystals because the state of powdered crystals is more close to the equilibrium than one of defected and stressed crystal aggregates.

The calculated values of parameters (α_i , θ_i) in Eq. (1) are presented in Table 3. Temperature dependence of relative deviation

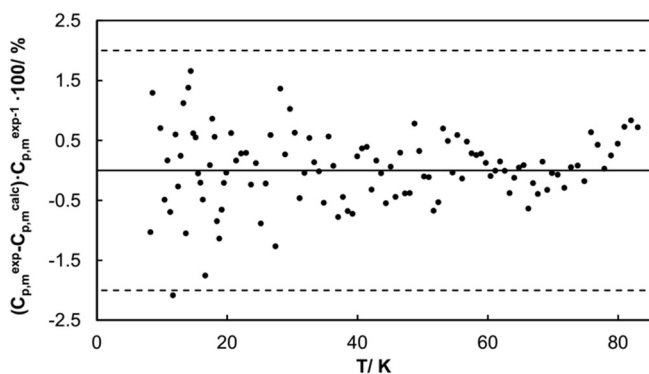


Fig. 10. Relative deviations (●) of the experimental heat capacity ($C_{p,m}^{\text{exp}}$) of $(\text{NH}_4)_2\text{Mg}(\text{SO}_4)_2 \cdot 6\text{H}_2\text{O}$ powdered crystals from calculated ($C_{p,m}^{\text{calc}}$) by Eq. (1) in the temperature range from 8 to 80 K. Dashed lines represents the declared instrumental error [15].

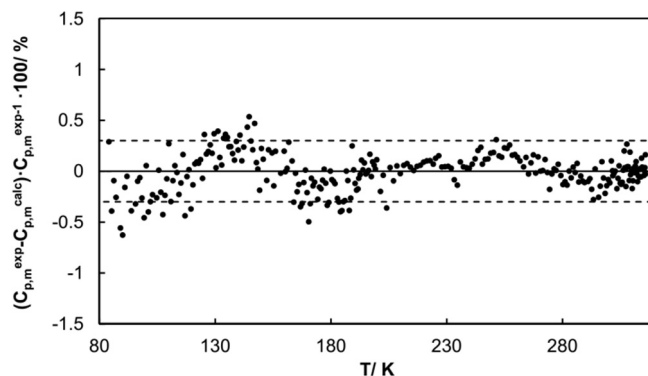


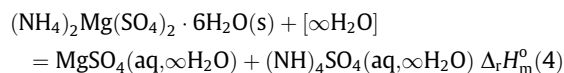
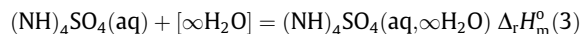
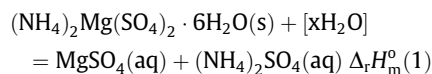
Fig. 11. Relative deviations (●) of the experimental heat capacity ($C_{p,m}^{\text{exp}}$) of $(\text{NH}_4)_2\text{Mg}(\text{SO}_4)_2 \cdot 6\text{H}_2\text{O}$ powdered crystals from calculated ($C_{p,m}^{\text{calc}}$) by Eq. (1) in the temperature range from 80 to 320 K. Dashed lines represents the declared instrumental error [15].

between experimental ($C_{p,m}^{\text{exp}}$) and calculated ($C_{p,m}^{\text{calc}}$) heat capacity are shown in Figs. 10 and 11. Standard relative deviation is 0.4%; maximum relative deviation is 2.1% at 11.65 K. Six Einstein functions are sufficient to approximate the molar heat capacity of $(\text{NH}_4)_2\text{Mg}(\text{SO}_4)_2 \cdot 6\text{H}_2\text{O}$. Reducing the number of terms in Eq. (1) lead to an appreciable deterioration in the quality of fitting; the statistical characteristics of fitting is improved insignificantly when the number of parameters is increased. Smoothed molar thermodynamic functions calculated by Eqs. (1)(3) are presented in Table 4.

4.4. Enthalpy of dissolution and functions of $(\text{NH}_4)_2\text{Mg}(\text{SO}_4)_2 \cdot 6\text{H}_2\text{O}$ formation

The results of calorimetric measurements of $(\text{NH}_4)_2\text{Mg}(\text{SO}_4)_2 \cdot 6\text{H}_2\text{O}$ dissolution in water are shown in Table 5.

We calculated the enthalpies of dissolution of $(\text{NH}_4)_2\text{Mg}(\text{SO}_4)_2 \cdot 6\text{H}_2\text{O}$ in water at infinite dilution using the experimental results on the enthalpy of dissolution of $(\text{NH}_4)_2\text{Mg}(\text{SO}_4)_2 \cdot 6\text{H}_2\text{O}$ in water and literary data on the enthalpies of dilution of aqueous solution of MgSO_4 and $(\text{NH}_4)_2\text{SO}_4$ [20]:



$$\Delta_r H_m^0(4) = \Delta_r H_m^0(1) + \Delta_r H_m^0(2) + \Delta_r H_m^0(3)$$

Values of reaction enthalpies $\Delta_r H_m^0(1) - \Delta_r H_m^0(4)$ are presented in Table 5. Values of $\Delta_r H_m^0(4)$ correspond to enthalpy of $(\text{NH}_4)_2\text{Mg}(\text{SO}_4)_2 \cdot 6\text{H}_2\text{O}$ dissolution at infinite dilution $\Delta_{\text{sol}} H_m^0$. $\langle \Delta_{\text{sol}} H_m^0 \rangle = (38.62 \pm 0.33) \text{ kJ} \cdot \text{mol}^{-1}$ is the average enthalpy of $(\text{NH}_4)_2\text{Mg}(\text{SO}_4)_2 \cdot 6\text{H}_2\text{O}$ dissolution (Expanded uncertainty $U(k = 2)$ of $\langle \Delta_{\text{sol}} H_m^0 \rangle$ is $0.3 \text{ kJ} \cdot \text{mol}^{-1}$).

The enthalpy of mixing of aqueous solution of MgSO_4 and $(\text{NH}_4)_2\text{SO}_4$ can be ignored, because the amount of these salts in solutions is insignificant against the large excess of water (1 mol salt in $13453 \div 15711 \text{ mol H}_2\text{O}$).

Table 4
Smoothed molar thermodynamic functions of $(\text{NH}_4)_2\text{Mg}(\text{SO}_4)_2 \cdot 6\text{H}_2\text{O}$; $P = 101.3 \text{ kPa}$; $R = 8.3144598 \text{ J} \cdot \text{mol}^{-1} \cdot \text{K}^{-1}$. These values were obtained from the heat capacity measurements of $(\text{NH}_4)_2\text{Mg}(\text{SO}_4)_2 \cdot 6\text{H}_2\text{O}$ powdered crystals.

T/K	$C_{p,m}/R$	$u(C_{p,m}/R)^b$	$(H_m^0(T) - H_m^0(0))/RT^b$	$u((H_m^0(T) - H_m^0(0))/RT)^b$	$S_m^0(T)/R$	$u(S_m^0(T)/R)^b$
5	0.050	0.001	0.016	0.004	0.02	0.01
10	0.163	0.003	0.053	0.02	0.08	0.02
15	0.71	0.01	0.17	0.03	0.2	0.1
20	1.67	0.03	0.4	0.1	0.6	0.1
25	2.9	0.1	0.8	0.1	1.1	0.1
30	4.3	0.1	1.2	0.2	1.7	0.2
35	5.8	0.1	1.8	0.2	2.5	0.3
40	7.4	0.1	2.4	0.3	3.3	0.3
45	9.0	0.2	3.0	0.3	4.3	0.4
50	10.6	0.2	3.7	0.4	5.3	0.5
55	12.2	0.2	4.4	0.5	6.4	0.5
60	13.8	0.3	5.1	0.5	7.5	0.6
65	15.4	0.3	5.8	0.6	8.7	0.7
70	16.9	0.3	6.6	0.6	9.9	0.7
75	18.4	0.4	7.3	0.7	11.1	0.8
80	19.8	0.4	8.1	0.8	12.4	0.8
90	22.6	0.1	9.5	0.1	14.9	0.2
100	25.2	0.1	11.0	0.2	17.4	0.2
110	27.7	0.1	12.4	0.2	19.9	0.2
120	30.0	0.1	13.7	0.2	22.4	0.2
130	32.2	0.1	15.1	0.2	24.9	0.3
140	34.3	0.1	16.4	0.2	27.4	0.3
150	36.2	0.1	17.6	0.2	29.8	0.3
160	38.1	0.1	18.9	0.2	32.2	0.3
170	40.0	0.1	20.0	0.2	34.6	0.3
180	41.7	0.1	21.2	0.3	36.9	0.3
190	43.5	0.1	22.3	0.3	39.2	0.3
200	45.2	0.1	23.4	0.3	41.5	0.3
210	46.9	0.1	24.5	0.3	43.7	0.4
220	48.6	0.1	25.6	0.3	45.9	0.4
230	50.3	0.2	26.6	0.3	48.1	0.4
240	51.9	0.2	27.6	0.3	50.3	0.4
250	53.5	0.2	28.6	0.3	52.5	0.4
260	55.1	0.2	29.6	0.3	54.6	0.4
270	56.7	0.2	30.6	0.3	56.7	0.4
280	58.3	0.2	31.5	0.4	58.8	0.4
290	59.7	0.2	32.5	0.4	60.9	0.5
298.15	60.9	0.2	33.3	0.4	62.5	0.5
300	61.2	0.2	33.4	0.4	62.9	0.5
310	62.6	0.2	34.3	0.4	64.9	0.5
320	64.1	0.2	35.3	0.4	66.9	0.5

^a Expanded uncertainties U ($k = 2$) are $U(T) = 0.02 \text{ K}$, $U(P) = 0.5 \text{ kPa}$.

^b Deviations u of the thermodynamic functions $C_{p,m}/R$, $(H_m^0(T) - H_m^0(0))/RT$ and $S_m^0(T)/R$ are standard uncertainties.

Table 5
Results of the measurements of the $(\text{NH}_4)_2\text{Mg}(\text{SO}_4)_2 \cdot 6\text{H}_2\text{O}$ enthalpy dissolution in water at $T = 298.15 \text{ K}$; $P = 101.3 \text{ kPa}$.^a

N_0	$-\Delta R/\Omega$	Q/J	Solvent quantity/g	m/g	$\Delta_r H_m^0(i)/\text{kJ} \cdot \text{mol}^{-1}$			
					$i = 1$	$i = 2$	$i = 3$	$i = 4$
1	0.03695	11.921	80	0.10666	40.30	-1.36	-0.63	38.31
2	0.03540	11.421	80	0.10196	40.39	-1.32	-0.63	38.44
3	0.03722	12.008	80	0.10638	40.70	-1.35	-0.63	38.72
4	0.04172	13.460	80	0.11908	40.76	-1.43	-0.69	38.64
5	0.03743	12.076	80	0.10634	40.95	-1.35	-0.63	38.97
Average value of $\langle \Delta_{\text{sol}} H_m^0 \rangle / \text{kJ} \cdot \text{mol}^{-1}$								38.62 ± 0.33 ^b

^a ΔR is the corrected temperature rise, Q is the energy absorbed in each experiment, m is the sample mass, $\Delta_{\text{sol}} H_m^0$ is the molar enthalpy change of the dissolution. $\Delta_r H_m^0(i)$ is the molar enthalpy of reaction (i): $i = 1, 4$ are the molar enthalpies of $(\text{NH}_4)_2\text{Mg}(\text{SO}_4)_2 \cdot 6\text{H}_2\text{O}$ dissolution in water ($i = 1$ – experimental data, $i = 4$ – at infinite dilution); $i = 2, 3$ are the enthalpies of dilution of aqueous solutions from experimental concentration to infinite dilution ($i = 2$ – $\text{MgSO}_4(\text{aq})$ and $i = 3$ – $(\text{NH}_4)_2\text{SO}_4(\text{aq})$) [20]. Expanded uncertainties U ($k = 2$) are $U(T) = 0.005 \text{ K}$; $U(P) = 0.5 \text{ kPa}$; $U(\Delta R) = 3 \cdot 10^{-5} \text{ K}$; $U(Q) = 0.009 \text{ J}$; $U(m) = 2 \cdot 10^{-5} \text{ g}$; $U(\text{Solvent quantity}) = 0.003 \text{ g}$.

^b Deviation of $\langle \Delta_{\text{sol}} H_m^0 \rangle$ is expanded uncertainty U ($k = 2$).

Table 6
Standard thermodynamic functions of $(\text{NH}_4)_2\text{Mg}(\text{SO}_4)_2 \cdot 6\text{H}_2\text{O}$ in the crystal state at $T = 298.15 \text{ K}$, $P = 101.3 \text{ kPa}$.^a

$C_{p,m}^0 / \text{J} \cdot \text{mol}^{-1} \cdot \text{K}^{-1b}$	$S_m^0 / \text{J} \cdot \text{mol}^{-1} \cdot \text{K}^{-1}$	$H_m^0(298.15) - H_m^0(0) / \text{kJ} \cdot \text{mol}^{-1}$	$\Delta_r S_m^0 / \text{J} \cdot \text{mol}^{-1} \cdot \text{K}^{-1c}$	$\Delta_r H_m^0 / \text{kJ} \cdot \text{mol}^{-1}$	$\Delta_r G_m^0 / \text{kJ} \cdot \text{mol}^{-1}$
507 ± 2	520 ± 4	82.4 ± 0.7	-2511.4 ± 0.2	-4306 ± 1	-3557 ± 1

^a Expanded uncertainty U ($k = 2$) is $U(T) = 0.02 \text{ K}$; $U(P) = 0.5 \text{ kPa}$.

^b Deviations of the thermodynamic functions are expanded uncertainties U ($k = 2$).

^c $\Delta_r S_m^0$ was calculated from S_m^0 of $(\text{NH}_4)_2\text{Mg}(\text{SO}_4)_2 \cdot 6\text{H}_2\text{O}$ and standard entropies of $\text{N}_{2(\text{g})}$, $\text{H}_{2(\text{g})}$, $\text{S}_{(\text{s})}$, $\text{O}_{2(\text{g})}$, $\text{Mg}_{(\text{s})}$ at the pressure 10^5 Pa [29].

The value of $(\text{NH}_4)_2\text{Mg}(\text{SO}_4)_2 \cdot 6\text{H}_2\text{O}$ enthalpy formation was calculated by Hess law as:

$$\begin{aligned} \Delta_f H_m^0((\text{NH}_4)_2\text{Mg}(\text{SO}_4)_2 \cdot 6\text{H}_2\text{O}, \text{s}) &= \Delta_f H_m^0(\text{Mg}^{2+}, \text{aq}) + 2\Delta_f H_m^0(\text{NH}_4^+, \text{aq}) \\ &\quad + 2\Delta_f H_m^0(\text{SO}_4^{2-}, \text{aq}) + 6\Delta_f H_m^0(\text{H}_2\text{O}, \text{l}) \\ &\quad - \Delta_{\text{sol}} H_m^0((\text{NH}_4)_2\text{Mg}(\text{SO}_4)_2 \cdot 6\text{H}_2\text{O}) \\ &= (-467.0 \pm 0.6) + 2(-133.26 \pm 0.25) \\ &\quad + 2(-909.34 \pm 0.40) \\ &\quad + 6(-285.83 \pm 0.04) - (38.62 \pm 0.33) \\ &= -(4305.8 \pm 1.2) \text{ kJ} \cdot \text{mol}^{-1}. \end{aligned}$$

Values of standard enthalpy of formation at 298.15 K for ions and water (first four members in the last formula) were taken from [30]. The overall expanded uncertainty ($k = 2$) of $(\text{NH}_4)_2\text{Mg}(\text{SO}_4)_2 \cdot 6\text{H}_2\text{O}$ enthalpy formation were calculated by equation $U = (\sum U_i^2)^{1/2}$, where U_i are the expanded uncertainties ($k = 2$) of values used in calculations. Standard thermodynamic functions of $(\text{NH}_4)_2\text{Mg}(\text{SO}_4)_2 \cdot 6\text{H}_2\text{O}$ are presented in Table 6.

Single data on the standard enthalpy of $(\text{NH}_4)_2\text{Mg}(\text{SO}_4)_2 \cdot 6\text{H}_2\text{O}$ formation at 298.15 K are reported in the literature [6]. This value was evaluated theoretically using a method developed by Viellard et al. [30]. $\Delta_f H_m^0$ for $(\text{NH}_4)_2\text{Mg}(\text{SO}_4)_2 \cdot 6\text{H}_2\text{O}$ obtained in the present study differs from the value estimated by [6] on 0.8%. We recommend to use standard enthalpy of $(\text{NH}_4)_2\text{Mg}(\text{SO}_4)_2 \cdot 6\text{H}_2\text{O}$ formation determined in the present work as reference, because this value was calculated from direct calorimetric measurements. However, it should be noted that the method developed by Viellard et al. [31] predicts enthalpies of formation of double salts hydrates with satisfactory accuracy.

5. Conclusions

Ammonium magnesium sulfate hexahydrate $(\text{NH}_4)_2\text{Mg}(\text{SO}_4)_2 \cdot 6\text{H}_2\text{O}$ was synthesized and characterized for subsequent complex experimental investigation. Thermal stability of the salt was evaluated at atmospheric pressure by DSC and TG methods. It was shown that melting parameters of the $(\text{NH}_4)_2\text{Mg}(\text{SO}_4)_2 \cdot 6\text{H}_2\text{O}$ obtained previously by Voight et al. [5] are incorrect. Incongruent melting temperature of the salt was estimated at external pressure 10^4 kPa by DSC. Solid products of $(\text{NH}_4)_2\text{Mg}(\text{SO}_4)_2 \cdot 6\text{H}_2\text{O}$ thermal decomposition are efremovite and ammonium sulfate; they were identified by DSC and XRD. Phase transition of $(\text{NH}_4)_2\text{Mg}(\text{SO}_4)_2 \cdot 6\text{H}_2\text{O}$ crystal aggregates was detected by means of DSC, AC and dielectric permittivity measurements. It was shown that this transition is absent for $(\text{NH}_4)_2\text{Mg}(\text{SO}_4)_2 \cdot 6\text{H}_2\text{O}$ having smaller crystal size obtained by grinding of the raw crystal aggregates in an agate mortar. Additional researches by other methods are needed to determine the nature of this phase transition. The thermodynamic properties of $(\text{NH}_4)_2\text{Mg}(\text{SO}_4)_2 \cdot 6\text{H}_2\text{O}$ were obtained by means of experimental methods for the first time. Temperature dependence of the $(\text{NH}_4)_2\text{Mg}(\text{SO}_4)_2 \cdot 6\text{H}_2\text{O}$ heat capacity was determined by AC from 8 to 320 K; results of experiment were approximated with a combination of Plank-Einstein functions. Enthalpy of $(\text{NH}_4)_2\text{Mg}(\text{SO}_4)_2 \cdot 6\text{H}_2\text{O}$ dissolution in water was measured by solution calorimetry method. The main thermodynamic functions ($C_{p,m}(T)$; $H_m^0(T) - H_m^0(0)$; $S_m^0(T)$) and functions of formation ($\Delta_f H_m^0$; $\Delta_f S_m^0$; $\Delta_f G_m^0$) of $(\text{NH}_4)_2\text{Mg}(\text{SO}_4)_2 \cdot 6\text{H}_2\text{O}$ were calculated from experimental and literature data. It was shown that the value of the standard enthalpy of formation determined in the present study is in a good agreement with the value predicted by Billon and Viellard [6].

Data obtained in the present study can be used further in the thermodynamic modeling of various systems with $(\text{NH}_4)_2\text{Mg}(\text{SO}_4)_2 \cdot 6\text{H}_2\text{O}$ hydrate as a constituent.

Acknowledgments

The work was performed at the User Facilities Center of Lomonosov MSU. The investigations were supported by the URALCHEM OJSC. The authors acknowledge partial support from the Lomonosov MSU Program of Development. Authors gratefully acknowledge Konstantin Zakharov for the dielectric permittivity measurements.

Appendix A. Supplementary data

Supplementary data associated with this article can be found, in the online version, at <https://doi.org/10.1016/j.jct.2017.11.016>.

References

- [1] N. Shimobayashi, M. Ohnishi, H. Miura, Ammonium sulfate minerals from Mikasa, Hokkaido, Japan: boussingaultite, godovikovite, efremovite and tschermigite, *J. Mineral. Petrol. Sci.* 106 (2011) 158–163, <https://doi.org/10.2465/jmps.101021f>.
- [2] J. Highfield, H. Lim, J. Fagerlund, R. Zevenhoven, Activation of serpentine for CO_2 mineralization by flux extraction of soluble magnesium salts using ammonium sulfate, *RSC Adv.* 2 (2012) 6535–6541, <https://doi.org/10.1039/c2ra01347a>.
- [3] M.M. Abd-Elzaher, Investigation of the reaction of roasted serpentine ore with some ammonium salts, *J. Chin. Chem. Soc.* 46 (1999) 975–982, <https://doi.org/10.1002/jccs.199900135>.
- [4] E.G. Neitzel Ulrich, Process for the production of anhydrous potassium magnesium sulfate material with low hygroscopicity from hydrated potassium magnesium sulfate material, U.S. Patent No. 3,617,243, 2 Nov. 1971.
- [5] W. Voigt, S. Goring, Melting of Tutton's salts studied by DSC, *Thermochim. Acta.* 231 (1994) 13–126, [https://doi.org/10.1016/0040-6031\(94\)85179-4](https://doi.org/10.1016/0040-6031(94)85179-4).
- [6] S. Billon, P. Viellard, Prediction of enthalpies of formation of hydrous sulfates, *Am. Mineral.* 100 (2015) 615–627, <https://doi.org/10.2138/am-2015-4925>.
- [7] A. Weston, CXLVI. The quaternary system potassium sulphate-magnesium sulphate-ammonium sulphate-water, *J. Chem. Soc., Trans.* 121 (1922) 1223–1237.
- [8] A. Benrath, W. Thiemann, Über die Polythermen der ternären Systeme, die neben Wasser je ein Sulfat der Alkalien und der Vitriolbildner enthalten, VII, *Zeitschrift für anorganische und allgemeine Chemie.* 208 (1932) 177–193, <https://doi.org/10.1002/zaac.19322080209>.
- [9] V.G. Shevchuk, L.L. Kost', Phase equilibria in the systems $\text{Cs}_2\text{SO}_4\text{-MgSO}_4\text{-H}_2\text{O}$ and $(\text{NH}_4)_2\text{SO}_4\text{-MgSO}_4\text{-H}_2\text{O}$ at 35 °C, *Russ. J. Inorg. Chem.* 9 (1964) 432–435 (in Russian).
- [10] V.I. Pilipchenko, V.G. Shevchuk, System $\text{Na}_2\text{SO}_4\text{-(NH}_4)_2\text{SO}_4\text{-MgSO}_4\text{-H}_2\text{O}$ at 50 °C, *Russ. J. Inorg. Chem.* 14 (1969) 828–831 (in Russian).
- [11] H. Montgomery, E.C. Lingafelter, The crystal structure of Tutton's salts. II. Magnesium ammonium sulfate hexahydrate and nickel ammonium sulfate hexahydrate, *Acta Cryst.* 17 (1964) 1478–1479, <https://doi.org/10.1107/S0365110X6400367X>.
- [12] D.A. Kosova, A.L. Emelina, M.A. Bykov, Phase transitions of some sulfur-containing ammonium salts, *Thermochim. Acta* 595 (2014) 51–60, <https://doi.org/10.1016/j.tca.2014.08.035>.
- [13] M.E. Wieser, M. Berglund, Atomic weights of the elements 2007 (IUPAC Technical Report), *Pure Appl. Chem.* 81 (2009) 2131–2156, <https://doi.org/10.1351/PAC-REP-09-08-03>.
- [14] M.E. Wieser et al., Atomic weights of the elements 2011 (IUPAC Technical Report), *Pure Appl. Chem.* 85 (2013) 1047–1078, <https://doi.org/10.1351/PAC-REP-13-03-02>.
- [15] R.M. Varushchenko, A.I. Druzhinina, E.L. Sorkin, Low-temperature heat capacity of 1-bromoperfluorooctane, *J. Chem. Thermodyn.* 29 (1997) 623–637, <https://doi.org/10.1006/jcht.1996.0173>.
- [16] R. Stevens, J. Boerio-Goates, A heat capacity of copper on the ITS-90 temperature scale using adiabatic calorimetry, *J. Chem. Thermodyn.* 36 (2004) 857–863, <https://doi.org/10.1016/j.jct.2004.06.008>.
- [17] T.B. Douglas, G.T. Furukawa, R.E. McCoskey, A.F. Ball, *Calorimetric properties of normal heptane from 0 to 520 K*, *J. Res. Natl. Bur. Stand.* 53 (1954) 139–153.
- [18] A.S. Monayenkova, S.A. Lezhava, A.A. Popova, L.A. Tiphlova, Enthalpy of formation of the yttrium ion in aqueous solution at infinite dilution, *J. Chem. Thermodyn.* 33 (2001) 1679–1686, <https://doi.org/10.1006/jcht.2001.0887>.
- [19] A.S. Monayenkova, A.F. Vorob'ev, A.A. Popova, L.A. Tiphlova, Thermochemistry of some barium compounds, *J. Chem. Thermodyn.* 34 (2002) 1777–1785, [https://doi.org/10.1016/S0021-9614\(02\)00171-4](https://doi.org/10.1016/S0021-9614(02)00171-4).
- [20] V.P. Glushko, *Termicheskie Konstanty Veshchestv (Thermal Constants of Substances)*, issue1–10, VINITI, Moscow, 1981.
- [21] R.O. Grishchenko, A.L. Emelina, P.Y. Makarov, Thermodynamic properties and thermal behavior of Friedel's salt, *Thermochim. Acta* 570 (2013) 74–79, <https://doi.org/10.1016/j.tca.2013.07.030>.
- [22] D. Batuk, M. Batuk, D.S. Filimonov, K.V. Zakharov, O.S. Volkova, A. Vasiliev, O.A. Tyablikov, J. Hadermann, A.M. Abakumov, Crystal structure, defects, magnetic and dielectric properties of the 2 layered $\text{Bi}_{3n+1}\text{Ti}_7\text{Fe}_{3n-3}\text{O}_{9n+11}$ perovskite-

- anatase intergrowths, *Inorg. Chem.* 56 (2017) 931–942, <https://doi.org/10.1021/acs.inorgchem.6b02559>.
- [23] D. Fox, M.M. Labes, A. Weissberger, *Physics and Chemistry of the Organic Solid State*, London, Interscience, New York, 1965, pp. 111–116.
- [24] J. De Bruijn, A. Dworkin, H. Szwarc, J. Godard, R. Ceolin, C. Fabre, A. Rassat, Thermodynamic properties of a single crystal of fullerene C₆₀: a DSC study, *Europhys. Lett.* 24 (1993) 551–556, <https://doi.org/10.1209/0295-5075/24/7/008>.
- [25] Y. Miyazaki, M. Sorai, R. Lin, A. Dworkin, H. Szwarc, J. Godard, Heat capacity of a giant single crystal of C₆₀, *Chem. Phys. Lett.* 305 (1999) 293–297, [https://doi.org/10.1016/S0009-2614\(99\)00391-7](https://doi.org/10.1016/S0009-2614(99)00391-7).
- [26] J.E. Fischer, D.E. Luzzi, K. Kniáz, A.R. McGhie, D.A. Ricketts-Foot, W.R. Romanow, R.M. Strongin, Existence of high-order superlattices in orientationally ordered C₆₀, *Phys. Rev. B.* 47 (1993) 14614–14617, <https://doi.org/10.1103/PhysRevB.47.14614>.
- [27] B. Hertweck, T. Armbruster, E. Libowitzky, Multiple phase transitions of leonite-type compounds: optical, calorimetric, and X-ray data, *Mineral. Petrol.* 75 (2002) 245–259, <https://doi.org/10.1007/s007100200027>.
- [28] G.F. Voronin, I.B. Kutsenok, Universal method for approximating the standard thermodynamic functions of solids, *J. Chem. Eng. Data* 58 (2013) 2083–2094, <https://doi.org/10.1021/je400316m>.
- [29] <http://td.chem.msu.ru/en/developments/cpfit/>.
- [30] J.D. Cox, D.D. Wagman, V.A. Medvedev, *CODATA. Key Values for Thermodynamics*, New York, London, Hemisphere, 1989.
- [31] P. Vieillard, Y. Tardy, Estimation of enthalpies of formation of minerals based on their refined crystal structures, *Am. J. Sci.* 288 (1988) 997–1040, <https://doi.org/10.2475/ajs.288.10.997>.

JCT 17-281